Journal of Physics: Conference Series

PAPER • OPEN ACCESS

Volume and bond length dependences of the electronic structure of 6-fold and 8-fold coordinated Co^{2+} in pressure transformed CoF_2

To cite this article: J.A. Barreda-Argüeso *et al* 2017 *J. Phys.: Conf. Ser.* **950** 042016

AIRAPT IOP Publishing
IOP Conf. Series: Journal of Physics: Conf. Series **950** (2017) 042016 doi:10.1088/1742-6596/950/4/042016

Volume and bond length dependences of the electronic structure of 6-fold and 8-fold coordinated Co^{2+} in pressure transformed CoF_2

J.A. Barreda-Argüeso [1], F. Aguado [1], J. González [1] , R. Valiente [2], L. Nataf [3], M.N. Sanz-Ortiz [1,4], F. Rodríguez [1,*]

[1] MALTA Consolider Team, DCITIMAC, Facultad de Ciencias, Universidad de Cantabria, 39005 Santander, Spain

[2] MALTA Consolider Team, Dpt. Física Aplicada, Facultad de Ciencias, Universidad de Cantabria, Santander, Spain

[3] Synchrotron SOLEIL, L'Orme des Merisiers, Saint-Aubin, BP 48, 91192 Gif-sur-Yvette Cedex, France

[4] SCIC biomaGUNE, Parque tecnológico de San Sebastián, Guipúzcoa, Spain

* Corresponding author's e-mail: fernando.rodriguez@unican.es

Abstract. This work reports an optical absorption study on CoF_2 under high-pressure conditions in the 0-80 GPa range. A recent structural study[1] performed on the pressure-induced phase-transition sequence of CoF_2 reveals that this compound undergoes a structural transformation associated with a change of Co^{2+} coordination from 6 (rutile type) to 8 (fluorite type) at 15 GPa, what implies a profound change in the Co^{2+} electronic ground state associated with the inversion of *d* orbitals from ($t_{2g}^5e_g^2$) to ($e_g^4t_{2g}^3$). This allows us to explore the Co^{2+} electronic structure, and hence 10*Dq*, as a function of the density and the Co-F bond length in both CoF_6 (rutile phase) and CoF_8 (fluorite phase) coordinations. The results are compared with those obtained in $KCoF_3$ (perovskite) in a wide range of Co-F distances (from 2.04 to 1.83 Å).

1. Introduction

There is a lack of experimental studies devoted to investigate the volume/density and bond length (*R*) dependencies of the crystal-field *d*-orbital splitting e_g-t_{2g} (10*Dq*) in transition metal ions (*TM*) occupying high-symmetry crystallographic sites. The situation is even harder if different coordination geometries are involved. Although experimental studies on 10*Dq*(*R*) have been usually performed at ambient pressure on series of *TM* compounds with different crystal structure and composition [1-4], rest-of-lattice and compositional effects can significantly mask the actual bond-length dependence of the *TM* electronic structure [5]. High-pressure spectroscopy solves out this problem since the electronic structure of a given compound can be measured as a function of pressure and eventually of *V* and/or *R* provided that its structure as a function of pressure is known.

Although pioneering works by Drickamer *et al.* [6] dealt with that problem in a lot of *TM* oxides and halides, correlations between 10*Dq* and *V* were performed on *TM*-doped Al_2O_3 or MgO (*TM*: Ti, Cr, V) since the equation of state was known only for few materials at that time [6, 7]. However impurity systems pose a scale problem of whether the *TM*-ligand bond length and its variation with pressure are the same for the host (Al-O) and impurity (Cr-O) as for example in ruby (Al_2O_3: Cr^{3+}) [4,8-10]. Recent high-pressure studies by optical spectroscopy provided such correlations in pure *TM*-ion compounds: NiO [11] and $BiFeO_3$ [11, 12]. These studies gave evidence of $10Dq(V)$, and thus of $10Dq(R)$ dependences close to $V^{-5/3}$ and R^{-5}, respectively, given that in these compounds $R(P)$ scales as $V^{1/3}(P)$, and therefore both dependences obey the same power law, in agreement with crystal-field theory (CFT) predictions. This result is quite surprising since CFT in the point charge approximation is very simple and does not take explicitly into account the *TM*-ligand bonding [13-15]. Although efforts to justify the R^{-5} law have been done on the basis of ligand field theory [16,17] and by means of LCAO-type calculations, there is a lack of experimental studies aiming to validate whether CFT predictions on $10Dq$ apply for 1) different *TM* coordinations in the same crystal, *i.e.* 6-fold and 8-fold cubic coordinations in CoF_2; 2) the same coordination in different crystals, *i.e.* 6-fold coordination in CoF_2 and $KCoF_3$; and 3) a coordination change, *i.e.* $10Dq$(6-fold)/$10Dq$(8-fold) for the same R value.

This work reports an optical absorption study on CoF_2 under high-pressure conditions in the 0-80 GPa range. A recent structural study [18] performed on the pressure-induced phase-transition sequence of CoF_2 reveals that this compound undergoes a structural transformation associated with a change of Co^{2+} coordination from 6 (rutile type) to 8 (fluorite type) at 15 GPa, what implies a profound change in the Co^{2+} electronic ground state associated with inversion of *d* orbitals splitting from ($t_{2g}^5\, e_g^2$) to ($e_g^4\, t_{2g}^3$). This different ground state electronic configuration allows us to explore clearly the Co^{2+} electronic structure, and hence $10Dq$, as a function of the density and $R_{\text{Co-F}}$ in the two coordinations: CoF_6 (rutile phase) and CoF_8 (fluorite phase), taking the structural data reported elsewhere [18]. The results will be compared with those obtained in $KCoF_3$ where the 6-fold coordination of Co^{2+} in the perovskite structure is stable up to 80 GPa, thus providing the widest $10Dq(R)$ range ever measured in *TM* ions.

2. Experimental

2.1. Crystal structure and x-ray diffraction

Single crystals of CoF_2 and $KCoF_3$ grown by the Bridgman method according to methods described elsewhere [18]. At ambient conditions CoF_2 crystallizes in the tetragonal space group *P4₂/mnm* (rutile phase) [18] and $KCoF_3$ in the cubic *Pm3m* (perovskite phase) [19,20]. The evolution of the crystal structure of $KCoF_3$ with pressure was studied by angle dispersive x-ray diffraction (AXRD) on powdered samples using the 12.2.2 beamline at the *Advance Light Source* (ALS). Pressure was applied by means of a symmetric piston cylinder Diamond Anvil Cell (DAC). High pressure experiments on polycrystalline CoF_2 were performed in the *Materials Science and Powder Diffraction* beamline (BL04) at *ALBA* synchrotron using a Boehler-Almax DAC. In all experiments samples were loaded with several Ruby spheres (10 μm diameter) as pressure gauge [21] using methanol-ethanol-water and silicone oil as pressure transmitting media.

2.2. Optical Absorption and Raman Spectroscopy

Optical absorption and Raman experiments were performed on single-crystal plates of CoF_2 (90x80x14 μm^3) and $KCoF_3$ (100x80x20 μm^3) were used for high-pressure optical absorption experiments. The optical spectroscopy experiments were carried out in membrane and Almax- Boehler DACs. 200-μm-thick Inconel gaskets were preindented to 40 μm. 200-μm-diameter holes were perforated with a BETSA motorized electrical discharge machine. The DAC was loaded with a single crystal plate of CoF_2 or $KCoF_3$ and ruby microspheres (10 μm diameter) as pressure probes [21] using silicon oil as pressure-transmitting medium.

Optical absorption under high-pressure conditions was performed on a prototype fiber-optics microscope equipped with two 25× reflecting objectives mounted on two independent *x -y -z* translational stages for the microfocus beam and the collector objective, and a third independent *x -y -z* translational stage for the DAC holder. Optical absorption data and images were obtained simultaneously with the same device [22]. Spectra in the UV-VIS and NIR were recorded with Ocean Optics USB 2000 and NIRQUEST 512 monochromators using Si- and InGaAs-CCD detectors, respectively.

Unpolarized micro-Raman scattering measurements were performed with a triple monochromator Horiba-Jobin-Yvon T64000 spectrometer in subtractive mode backscattering configuration, equipped with an Horiba Symphony liquid-nitrogen-cooled CCD detector. The 514.5-nm and 647-nm lines of an Coherent Innova 70 Ar^+-Kr^+ laser were focused on the sample with a 20× objective for micro-Raman, and the laser power was kept below 4 mW in order to avoid heating effects. The laser spot was 20 μm in diameter and the spectral resolution was better than 1 cm^{-1}. The Raman technique was used in combination with X-ray diffraction to check the sample structure through the characteristic first-order modes in CoF_2 [18] and absence of first-order modes in $KCoF_3$ as well as to determine structural phase-transition pressures. The Raman high-pressure experiments were performed on the same CoF_2 and $KCoF_3$ single crystals employed in the optical absorption measurements.

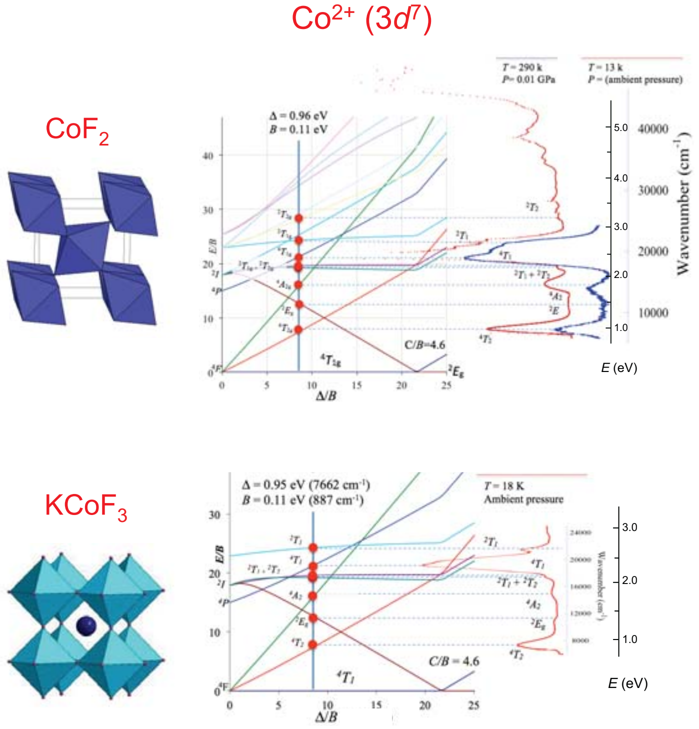

Figure 1. Optical absorption spectra of CoF_2 and $KCoF_3$ at ambient pressure and 290 K and low temperature (13 and 18 K, respectively). Spectra are normalized to the absorption coefficient. The peak energies are compared with those predicted by the Tanabe-Sugano diagram for octahedral Co^{2+} ($3d^7$): Racah (B) and crystal-field ($10Dq$) parameters obtained by fitting the experimental energies to the calculated energies are: $\Delta = 0.950\pm0.005$ eV and $B = 0.105\pm0.003$ eV for $KCoF_3$; and $\Delta = 0.962\pm0.005$ eV and $B = 0.107\pm0.003$ eV for CoF_2 ($\Delta/B = 9$).

3. Results and discussion

Figure 1 shows the electronic absorption spectrum of CoF_2 and $KCoF_3$ at ambient pressure, as well as the Tanabe-Sugano and corresponding B and $10Dq$ parameters, which account for the Co^{2+} transition energies. Both compounds exhibit a similar spectrum as it mainly corresponds to the CoF_6 coordination unit with similar Co-F bond distances: R = 2.042 and 2.035 Å [23,24]; and associated CF parameters: B = 0.107 and 0.105 eV; and $10Dq$ = 0.962 and 0.950 eV, for CoF_2 and $KCoF_3$, respectively. Interestingly, the similarity of spectra strengthen the relevance of CoF_6 to account for the CF electronic structure of Co^{2+} beyond other ionic shells of the crystal, the influence of which seems to be much weaker than the first F^- shell in spite of the distinct crystal structure: rutile (CoF_2) and perovskite ($KCoF_3$). However, the slightly bigger $10Dq$ of CoF_2 with respect to $KCoF_3$ contrasts with the shorter Co-F distance in $KCoF_3$ must be ascribed to rest-of-the-lattice CF effects beyond CoF_6, which is estimated to be less than 4% of $10Dq$.

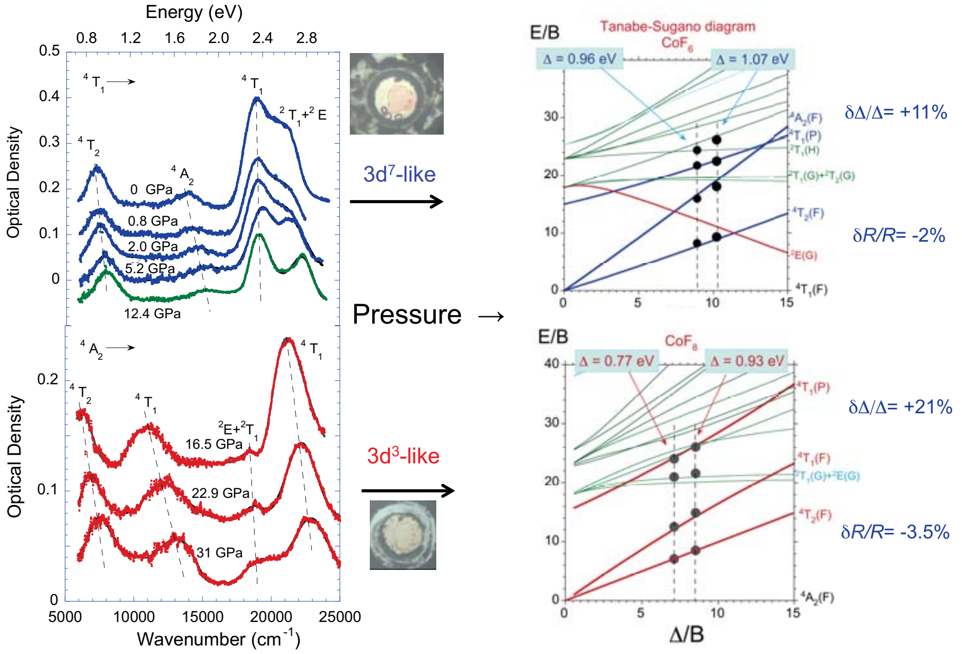

Figure 2. Pressure dependence of the optical absorption spectrum of CoF_2. Spectra correspond to rutile-type structure (blue), orthorhombic (green) with 6-fold coordinated Co^{2+}, and to fluorite-type phase (red) with 8-fold coordinated Co^{2+} [18]. The bands correspond to crystal-field transitions from the electronic ground state $^4T_1(F)$ in CoF_6 and $^4A_2(F)$ in CoF_8 to different excited states Γ_i according to the assignment given in the corresponding Tanabe-Sugano diagrams for d^7 and d^3, respectively. The energy of the Γ_i state is represented as a function of the crystal-field splitting and are both given in units of the Racah parameter B [24]. Colour representing Γ_i state has been maintained in both figures. The two sets of experimental points in the Tanabe-Sugano diagram denote the low pressure and high-pressure limits in both 6-fold and 8-fold coordinations. The relative crystal-field, $\Delta 10Dq$ / $10Dq$ (or $\delta\Delta/\Delta$), and corresponding $\delta R/R$ variations are given right side.

The variation of the absorption spectra with pressure for the two compounds is shown in figures 2 and 3. The extreme pressure points are represented in the Tanabe-Sugano diagram to illustrate the $10Dq/B$ range swept by pressure in each coordination: CoF_6 (d^7-like) or CoF_8 (d^3-like). The variations of $10Dq$ and R in the corresponding pressure range are also indicated. Interestingly, the CoF_6 (*rutile*) to CoF_8 (*fluorite*) change of coordination taking place in CoF_2 at 15 GPa induces a drastic change in the absorption spectrum which is associated with the corresponding change of electronic configuration (from d^7-like to d^3-like) affecting the ground and excited states, and hence the absorption spectra. However such an abrupt change is not observed in $KCoF_3$ since the CoF_6 octahedral coordination is stable in the 0 - 80 GPa range as indicated by AXRD experiments whose $V(P)$ data are represented in figure 3 (right). Consistently, the absorption spectrum of $KCoF_3$ in the whole pressure range is concomitant with an electronic configuration d^7 and thus the experiment provides the widest $10Dq(R)$ range explored ever in Co^{2+}.

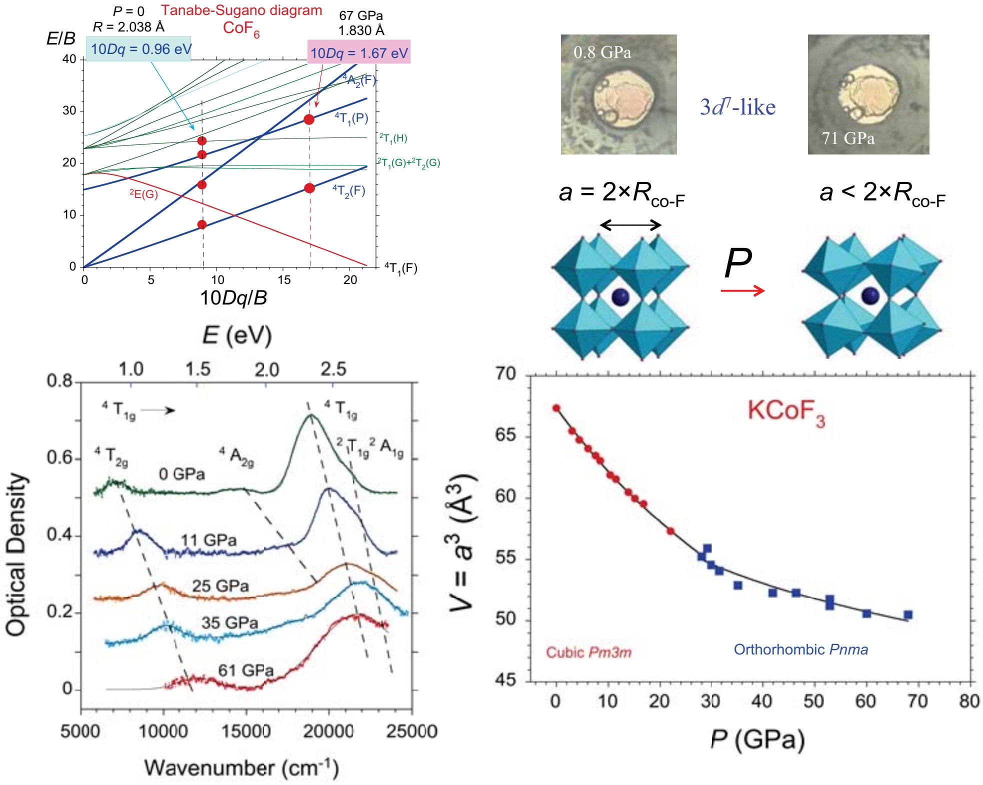

Figure 3. Variation of the absorption spectrum of $KCoF_3$ with pressure (left) and of the perovskite cell volume $V(P)$ (right). The peak energies are compared with those predicted by the Tanabe-Sugano diagram. The B and $10Dq$ parameters obtained by fitting the experimental energies $E(P)$ to the calculated crystal-field energies are: $10Dq = 0.960\pm0.005$ eV and 1.67 ± 0.01 eV, and $B = 0.105\pm0.003$ and 0.100 ± 0.003 eV for $KCoF_3$ at 0 and 67 GPa, respectively. The Tanabe Sugano-diagram compares the $10Dq/B$ range swept by pressure for CoF_6 in $KCoF_3$ (red dots): $10Dq/B = 10 \rightarrow 18$. The corresponding R variation obtained from the Equation of State $V(P)$ is indicated.

In general, pressure-induced phase transitions in both CoF_2 and $KCoF_3$ affect the electronic spectra as evidenced through their $10Dq(P)$ behaviour (figure 4). The different slope of $10Dq(P)$ exhibited by the perovskite $KCoF_3$ unravels the effect of a cubic (*Pm-3m*) to orthorhombic (*Pnma*) second-order phase transition at 24 GPa. Such a phase transition, which is associated with rotations of the CoF_6 octahedra, keeps the 6-fold octahedral coordination of Co^{2+} in the high-pressure orthorhombic phase, and thus $10Dq$ varies continuously at the phase transition, although its pressure dependence is different in each phase. This pressure behaviour contrasts with that exhibited by CoF_2, whose 10*Dq*(*P*) values show a peculiar pressure dependence through which the corresponding 10*Dq*(*R*) have been derived using the available XRD and XAS structural data reported elsewhere [18]. In CoF_2 pressure induces an increase of 10*Dq* from 0.96 to 1.06 eV in the 0-6 GPa (rutile phase), whereas at 15 GPa, it abruptly decreases by -0.3 eV along with the 6- to 8-fold coordination change. Above 15 GPa, 10*Dq* increases at a rate of 9 meV GPa^{-1} in the fluorite phase, and at 4.4 meV GPa^{-1} beyond 44 GPa in the cotunnite phase [18].

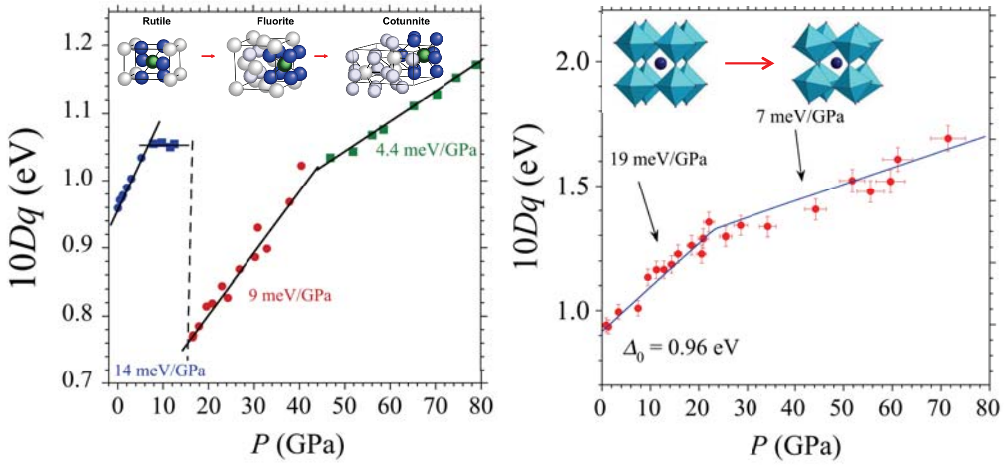

Figure 4. Variations of the Co^{2+} crystal-field splitting energy between e_g and t_{2g} *d*-orbitals with pressure in CoF_2 (left) and $KCoF_3$ (right). The coordination of Co^{2+} and the 10*Dq*(*P*) pressure shift are indicated for each crystal phase. Anomalies in 10*Dq*(*P*) observed at 6, 15 and 44 GPa in CoF_2, and at 24 GPa in $KCoF_3$, correspond to structural phase transitions $P4_2/mnm$ (rutile) ↔ *Pbca* ↔ *Fm3m* (fluorite) ↔ *Pnma* (cotunnite) in CoF_2, and *Pm3m* ↔ *Pnma* (perovskite) in $KCoF_3$, respectively.

4. Concluding remarks

The knowledge of EOS and *R*(*P*) in the two investigated compounds from XRD and XAS (Figure 3) [18,20] allows us to derive 10*Dq*(*R*) from the corresponding 10*Dq*(*P*). A noteworthy result concerns the regular variation of 10*Dq*(*R*) in CoF_6 and CoF_8 with respect to variations of 10*Dq*(*P*) that show anomalies at the phase transitions in both CoF_2 and $KCoF_3$. Such anomalies are concurrent with similar anomalies in *R*(*P*) thus highlighting the suitability of *R* (and neither *V* nor density) to properly describe pressure-induced variations of 10*Dq*. Furthermore 10*Dq*(*R*) obeys a potential law as R^{-n} with *n* close to 5 in both compounds. In particular, we get an exponent $n = 5.1 \pm 0.3$ in $KCoF_3$ in an *R* range of 12% whereas in CoF_2 $n = 5.0 \pm 0.1$ (rutile phase) and $n = 6.0 \pm 0.2$ (fluorite phase) as deduced from their relative changes of *R* and 10*Dq* in the explored *R*-ranges (figures 2 and 3).

The reliability of CFT to fairly account for *R*-dependence of 10*Dq* is also confirmed through the relative 10*Dq* values obtained for CoF_6 and CoF_8 in CoF_2 at the same Co-F distance, $R = 2.04$ Å, as $10Dq(oct)/10Dq(cub) = 1.10$. Its similitude with the theoretical value of 9/8 supports CFT predictions to accurately describe experimental 10*Dq*(*R*).

Finally, this study constitutes a reference system to validate *ab initio* methods aiming to calculate electronic structure (including excited states) of *TM* ions besides of well-suited DFT methods to calculate crystallographic and vibrational structures.

Acknowledgments

Financial support from the Spanish Ministerio de Economia y Competitividad (Project No. MAT2015-69508-P) and MALTA INGENIO-CONSOLIDER 2010 (Ref. No. CDS2007-0045) is acknowledged.

The ALS is supported by the Director, Office of Science, Office of Basic Energy Sciences of the US Department of Energy, under Contract No. DE-AC02-05CH11231.

References

[1] Rodríguez F and Moreno M 1986 *J. Phys. Chem.* **84** 692

[2] Grinberg M 2006 *Opt. Mat.* **28** 26

[3] Rodríguez-Lazcano Y, Nataf L, Rodríguez F 2009 *Phys. Rev. B* **80** 085115-1

[4] Marco-de-Lucas MC, Rodríguez F, Güdel HU, and Furer N 1994 *J. Lumin*. **60/61** 581

[5] García-Lastra J M, Barriuso M T, Aramburu J A, and Moreno M 2005 *Phys. Rev. B* **72** 113104

[6] Drickamer H G and Frank C W 1973 *Electronic structure, electronic transitions and the high pressure chemistry and physics of solids* (Chapman and Hall: London)

[7] Tonkov E Y 1992 *High Pressure Phase Transformations: A Handbook* (Gordon & Breach: Amsterdam)

[8] Duclos S D, Vohra Y K and Ruoff A L 1990 *Phys. Rev. B* **41** 5372

[9] Millot M, Broto J M, Gonzalez J and Rodríguez F 2010 *Phys. Rev. B* **81** 075120

[10] Duan W, Paiva G, Wentzcovitch R M and Fazzio A 1998 *Phys. Rev. Lett.* **81** 3267

[11] Gavriliuk A G, Trojan I A and Struzhkin V V 2012 *Phys. Rev. Lett.* **109** 086402

[12] Gomez-Salces S, Aguado F, Rodriguez F, Valiente R, Gonzalez J, Haumont R and Kreisel J 2012 *Phys. Rev. B* **85** 144109

[13] Lever A B P 1984 *Inorganic Electronic Spectroscopy* (Elsevier: Amsterdam)

[14] Burns R G 1993 *Mineralogical Applications of Crystal Field Theory* (Cambridge University Press: Cambridge)

[15] Griffith J S 1908 *The theory of Transition-Metal Ions* (Cambridge University Press: Cambridge)

[16] Curie D, Barthou C and Canny B 1974 *J. Chem. Phys.* **61** 3048

[17] Liu L, Li X D, Li Y C, Tang L Y, Liu J and Ban Y 2009 *Chin. J. High Press. Phys.* **23** 209

[18] Barreda-Argüeso J A, López-Moreno S, Sanz-Ortiz M N, Aguado F, Valiente R, González J, Rodríguez F, Romero A H, Muñoz A, Nataf L, and Baudelet F 2013 *Phys. Rev. B* **88** 214108

[19] Julliard J and Nouet J 1975 *Rev. Phys. Appl.* **10** 325

[20] Aguado F, Rodriguez F and Redfern S A T 2009 *High Pressure Res.* **29** 525

[21] Syassen K 2008 *High Pressure Res.* **28** 75

[22] Barreda-Argüeso J A and Rodríguez F 2014 *Microscopio para la caracterización espectroscópica de una muestra* (Patent PCT/ES2014/000049)

[23] Costa N M R, Paixao J A, De Almeida M J M and Andrade L C R 1993 *Acta Crystallogr. B* **49** 591

[24] Sugano S and Tanabe Y 1958 *J. Phys. Soc. Jpn.* **13** 880